IVYSPRING INTERNATIONAL PUBLISHER

International Journal of Biological Sciences

2023; 19(10): 3249-3265. doi: 10.7150/ijbs.81900

Research Paper

β-amyloid binds to microglia Dectin-1 to induce inflammatory response in the pathogenesis of Alzheimer's disease

Xia Zhao[1#], Jinfeng Sun[1,2#], Li Xiong[1], Lingyu She[2], Liwei Li[1], Hao Tang[1], Yuqing Zeng[1], Fan Chen[1], Xue Han[1], Shiju Ye[3], Wei Wang[1], Xu Wang[3,4], Guang Liang[1,3,✉]

1. Affiliated Yongkang First People's Hospital and School of Pharmacy, Hangzhou Medical College, Hangzhou, Zhejiang, 310012, China.
2. Key Laboratory of Natural Medicines of the Changbai Mountain, Ministry of Education, College of Pharmacy, Yanbian University, Yanji, Jilin, 133002, China.
3. Chemical Biology Research Center, School of Pharmaceutical Sciences, Wenzhou Medical University, Wenzhou, Zhejiang,325035, China.
4. Oujiang Laboratory (Zhejiang Lab for Regenerative Medicine, Vision and Brain Health); Wenzhou Medical University, Wenzhou, Zhejiang,325035, China.

[#] Equal contribution

✉ Corresponding author: Guang Liang, Ph.D., Professor. Address: Affiliated Yongkang First People's Hospital and School of Pharmacy, Hangzhou Medical College, Hangzhou, Zhejiang, 310012, China. E-mail: wzmcliangguang@163.com

Received: 2022.12.15; Accepted: 2023.06.15; Published: 2023.06.19

Abstract

Microglia-mediated neuroinflammation is closely related to the development of Alzheimer's disease (AD). In the early stages of the inflammation response, pattern recognition receptors (PRRs) play a key role in clearing damaged cells and defending against infection by recognizing endogenous and exogenous ligands. However, the regulation of pathogenic microglial activation and its role in AD pathology remains poorly understood. Here we showed that a pattern recognition receptor called Dectin-1, expressed on microglia, mediates the pro-inflammatory responses of beta-amyloid (Aβ). Knockout of Dectin-1 reduced Aβ1-42 ($A\beta_{42}$)-induced microglial activation, inflammatory responses, and synaptic and cognitive deficits in $A\beta_{42}$-infused AD mice. Similar results were obtained in the BV2 cell model. Mechanistically, we showed that $A\beta_{42}$ could directly bind to Dectin-1, causing Dectin-1 homodimerization and activating downstream spleen tyrosine kinase (Syk)/nuclear factor-κB (NF-κB) signaling pathway to induce the expression of inflammatory factors and, in turn, AD pathology. These results suggest the important role of microglia Dectin-1 as a new direct receptor for $A\beta_{42}$ in microglial activation and AD pathology and provide a potential therapeutic strategy for neuroinflammation in AD.

Keywords: β-amyloid; Dectin-1; Microglia; Neuroinflammation; Alzheimer's disease

Introduction

Alzheimer's disease (AD) is characterized by a progressive loss of memory and cognitive impairment. Although multiple pathological theories have been proposed, the underlying mechanism remains unclear, leading to ineffective treatments. Neuroinflammation is an early pathological change that drives the progression of AD [1]. Microglia, the resident mononuclear phagocytes of the central nervous system (CNS), are the main executors of immune functions in the brain [2]. Genome-wide association studies have shown that many AD risk genes are highly expressed in microglia and play important roles in the occurrence and development of AD [3]. Therefore, microglia are crucial in the early stages of AD and may be potential therapeutic targets. Beta-amyloid (Aβ) deposition is one of the most important pathological features of AD and is produced by the cleavage of amyloid precursor protein (APP) by β-secretase and γ-secretase [4]. Among amyloid-forming fragments, $A\beta_{42}$ is the most toxic and easily aggregates to form amyloid plaques [5]. Aβ can activate microglia, resulting in production

of inflammatory factors such as tumor necrosis factor (TNF)-α, interleukin (IL)-6, and IL-1β [6]. Injecting $A\beta_{42}$ into the mouse hippocampus can induce microglial activation and extensive inflammatory responses, causing significant effects on the central nervous system [7, 8]. In the brains of patients with AD, approximately 80% of the "amyloid plaque" structures are covered by activated microglia [9]. These studies indicate a key role for Aβ in microglial activation, neuroinflammation, and AD development. However, the precise mechanism and direct receptors by which Aβ induces inflammation in microglia are not fully understood.

Pattern recognition receptors (PRRs) play an important role in clearing damaged cells and defending against infection by recognizing endogenous and exogenous ligands [10]. Dectin-1 (encoded by *Clec7a* gene), a member of the C-type lectin family of PRRs, is expressed selectively in myeloid-monocytic lineage cells, including microglia [11]. Dectin-1 contains an extracellular C-like lectin domain (C-lectin domain), a transmembrane domain, and an intracytoplasmic tyrosine activation motif (ITAM). When Dectin-1 is activated by ligands, intracellular ITAM recruits spleen tyrosine kinase (Syk) to induce Syk phosphorylation, which further activates NF-κB to induce pro-inflammatory gene transcription [12]. The C-lectin domain in the extracellular segment plays the role of recognizing and binding ligands [13]. Originally, Dectin-1 was found to recognize β-glucans in fungal pathogens and elicit antifungal pro-inflammatory immune responses. Recent studies have shown that in addition to classical β-glucan ligands, Dectin-1 is also involved in non-pathogen-mediated sterile inflammation [14]. In the central nervous system, Dectin-1 is significantly increased upon exposure to various stimuli such as ischemia and injury [15]. In models of intracerebral hemorrhage, Dectin-1 has been shown to cause macrophage polarization, and the activated Syk/NF-κB pathway contributes to brain injury [15]. Dectin-1 antagonist treatment significantly reduces the number of activated microglia and the level of inflammation in ischemic brain tissue and OGD/R-treated microglia [16, 17]. In addition, activation of Dectin-1 leads to macrophage-mediated axonal damage, whereas blockade of Dectin-1 reduces inflammatory macrophage-mediated axonal damage after spinal cord injury [18]. These studies suggest that Dectin-1 plays an important role in neurological diseases. However, whether Dectin-1 is involved in Aβ-induced neuroinflammation and AD pathology is largely unknown. More importantly, endogenous ligands that activate Dectin-1 in the brain under sterile inflammatory conditions have not been identified.

In this study, we investigated the expression and function of Dectin-1 in an $A\beta_{42}$-infused model of AD. Our results showed that the knockout of Dectin-1 improved neuroinflammation, cognitive function, and neurological damage in $A\beta_{42}$-infused mice. Importantly, our detailed mechanistic studies in microglia revealed that Aβ directly binds to Dectin-1 to initiate Syk/NF-κB signaling and induce inflammatory cytokines. This study identified Dectin-1 as a novel non-classical Aβ receptor and suggested that it plays an important role in neuroinflammation and AD pathology.

Materials and Methods

General Reagents

Amyloid beta-peptide (1-42) (PA4391) was purchased from Ontores Biotechnologies (Zhejiang, China). Recombinant human Dectin-1 (rhDectin-1) was purchased from Sino Biological (10215-HNCH; Beijing, China). HA-tag (51064-2-AP) and Flag-tag (20543-1-AP) were ordered from Proteintech (Shanghai, China). Biotin (D8150) and Biotinylated-$A\beta_{42}$ (Bio-$A\beta_{42}$) was obtained from GL Biochem (Shanghai, China). Penicillin/Streptomycin and Opti-MEM were ordered from Gibco (Carlsbad, CA, USA). Annexin V-FITC/PI Apoptosis Detection Kit was purchased from BD Biosciences (San Diego, CA, USA). Bovine serum albumin (BSA), Dulbecco's modified Eagle's medium (DMEM) and Dimethyl sulfoxide (DMSO) were ordered from Sigma (St. Louis, MO, USA). MTT powder, reactive oxygen species assay kit (ROS), JC-1 assay kit, RIPA lysis buffer and Hoechst 33258 were bought from Beyotime Institute of Biotechnology (Shanghai, China). PVDF membrane, ECL Plus and Western Blot Marker were bought from Bio-Rad. The list of antibodies used and their source is presented in the supplementary information Table S1. Sequence Information of β-Amyloid (1-42) used in this study was shown in the Supplementary Information Table S2.

Experimental AD models and treatment

The experimental protocol was approved by Hangzhou Medical College Animal Ethics Committee (2022-001). D1KO male mice (18-22g) on a C57BL/6 background and wild type male C57BL/6 mice (18-22g) were ordered from GemPharmatech (Nanjing, China). The dectin-1 knockout allele lacks sequences corresponding to the cytoplasmic tail region, transmembrane region and stalk region of the Dectin-1 locus (*Clec7a*). All the mice were housed in Hangzhou Medical College Animal Research Center under 22-24°C, 60–65% humidity, 12 hours/dark-light cycle, and fed a standard rodent diet. Before initiating the studies, all the mice were acclimatized in the

laboratory for at least 2 weeks. We used two AD models in this study: $A\beta_{42}$ infusion AD Model and APP/PS1 (APPswe, PSEN1dE9) AD model.

$A\beta_{42}$ infusion AD Model

Eight-week-old Wide Type C57BL/6 mice (WT mice) and Dectin-$1^{-/-}$ on Wide Type background mice were randomly divided into four groups: WT (WT mice controls, n = 10), $A\beta_{42}$ ($A\beta_{42}$-infused WT mice; n = 10), D1KO (Dectin-$1^{-/-}$ mice controls; n = 10), and D1KO+$A\beta_{42}$ ($A\beta_{42}$-infused Dectin-$1^{-/-}$ mice; n = 10). $A\beta_{42}$ peptide was incubated at 37°C to aggregate for one week before use [19]. All the mice were anesthetized with an intraperitoneal injection of 1% pentobarbital (40 mg/kg) and fixed to a stereotactic apparatus. A single injection of the aggregated form of $A\beta_{42}$ (5μg/μL) was administered unilaterally into the right hippocampal CA1 molecular layer of the mice (2μL per mouse). The following injection site coordinates were determined based on the Paxinos and Franklin atlas [20]. The bregma is 0; the rear opening is 2.0 mm, the side opening is ± 1.5 mm, and the depth is 1.5 mm. After injection, the needle was kept in place for another 2 minutes and then pulled out slowly.

APP/PS1 (APPswe, PSEN1dE9) AD model:

APP/PS1 double transgenic mice were obtained from The Jackson Laboratory [B6; C3-Tg (APPswe, PSEN1dE9)85Dbo/Mmjax]. These mice are expressing a mutant human presenilin 1 (PS1-dE9) and a chimeric mouse/human amyloid precursor protein (Mo/HuAPP695swe), which directly target neurons in the central nervous system. Both mutations have been linked to early-onset Alzheimer's disease. These mice are widely used in studies of Alzheimer's disease [21]. Six-month-old Wide Type mice (n = 3); Six-month-old APP/PS1 mice (n = 3) were used for Western blotting and IF to detect Dectin-1 expression.

Morris water maze (MWM)

To test the effect of Dectin-1 on the memory and learning abilities of AD model mice, the Morris water maze was performed. Briefly, mice were tested for place navigation on 4 consecutive days followed by a spatial probe test (without platform) on the 5th day [22]. During the place navigation tests the platform was placed 1 cm below the water surface in the middle of the target quadrants. The time and movement route of the mice to find the platform were recorded. The above operation was repeated daily from the 2nd until the 4th day. On the 5th day, the platform was removed and the mice were allowed to swim freely for 60 s for spatial probe experiments. The time spent in the target quadrant and the number of crossings platform were recorded [23]. All data collection and processing were done by image automatic monitoring and processing system (VisuTrack, Shanghai China).

New Object Recognition (NOR)

The bottom surface of the mouse experimental device is a square of 25 × 25 cm, and the four walls are 40 cm high. Before the experiment, the mice of each group were moved to the test room to acclimate to the test environment. On the first day, two identical objects A were placed in the experimental setup. After the mice were put in, the video equipment was turned on to record the contact between the mice and the two objects, including the number of times they touched the objects and the time spent exploring within 2-3 cm from the objects. The test duration was 5 minutes. After 24 hours, replace one of the A objects with B objects, and record with video equipment for 5 minutes. Then analyze the cognition of the mice: if the mice have poor cognitive ability, there is no difference in the exploration of new and old objects; if the mice have normal cognitive ability, the exploration of new objects is longer than that of old objects. The cognitive index (recognition index, RI) is calculated as: RI = new object / (new object + old object) × 100 %.

Immunofluorescence (IF)

After post-fixation in 4% PFA for approximately 24 hours, the paraformaldehyde was replaced by 20% sucrose. After the samples sunk to the bottom of the container, the 20% sucrose was replaced by a 30% sucrose solution until the samples sinking. The brains were cut at a thickness of 20 μm using a low temperature thermostat (Leica CM3050, Germany). Each section was dried for 20 minutes and then washed with 1xPBS for three times. Non-specific binding was blocked with 10% bovine serum albumin for 60min at room temperature. After that, tissue sections were incubated with the corresponding primary antibodies at 4°C overnight. Next day, all the sections were incubated with appropriate secondary antibody for 1h at room temperature. All incubations were followed by three washes in PBS for 15 min. Nuclei were stained with DAPI (Sigma, D6578), and the images were acquired with a Nikon A1 confocal microscope.

ELISA assay

After behavior test, blood samples from each group of mice were collected. Serum was obtained by centrifuge at 12000 rpm for 10 min and the levels of TNF-α and IL-1β were measured using ELISA kits. Briefly, samples were added to the wells with a biotin-conjugated antibody specific to TNF-α or IL-1β. Then, Avidin conjugated to Horseradish Peroxidase

(HRP) was added to each microplate well and incubated. Then, TMB substrate solution was added and incubated, those wells that contain TNF-α or IL-1β, biotin-conjugated antibody and enzyme-conjugated Avidin exhibited a change in color. Finally, stop solution was added to stop the reaction and the color change were measured at a wavelength of 450 nm by a microplate reader. The concentration of TNF-α or IL-1β in the samples were then determined by comparing the OD value of the samples to the standard curve.

Immunocytochemistry (ICC)

Properly treated BV2 cells were fixed in 4% paraformaldehyde (PFA) for 15-20 min. The BV2 cells were then incubated with 1x PBS containing 0.1% Triton X-100 (PBST) for 20 min to increase membrane permeability. After block with 1% BSA for 1 h at room temperature, the primary antibody (1:100) was added and incubate overnight at 4 °C. Next day, the cells were washed three times with 1xPBS and incubated with fluorophore conjugated secondary antibody (1:500) for 2h. Finally, one drop of antifade mounting medium with DAPI (P0131, Beyotime) was added to stain the Nuclei. Then, sections were observed and analyzed under a Nikon A1 confocal microscope.

TUNEL staining

To test cellular apoptosis, TUNEL assay was performed (C1098, Beyotime, Shanghai, China). For cells: Properly treated BV2 cells were fixed with 4% PFA for 20 min and washed with PBST for 3 times. Then cells were incubated with TUNEL test solution (5 μl of TdT enzyme and 45 μl of fluorescent labeling solution) under dark condition for 1h. After washing with 1xPBS for three times, nuclei were stained with DAPI. The apoptotic cells (green fluorescence) were observed under fluorescent microscopy and calculated as a percentage of the total number of cells. For brain tissue: Processed tissue samples were incubated with 50 μl of TUNEL reaction mixture for 1h at 37°C under dark conditions. Color developed in DAB coloring solution. Apoptosis index (brown color) in the hippocampus area were measured using this formula: apoptosis index (%) = (apoptotic neurons / total neurons) × 100%.

Microglia Phagocytosis and Clearance Assay

BV2 cells were seeded in 12-well plates and divided into four groups: Ctrl, $A\beta_{42}$, siD1 and $A\beta_{42}$+siD1 group. Cells were transfected with Dectin-1 interference plasmid or control plasmid with liposome 2000 for 24 h. Then incubated with/without 20 μM FITC-$A\beta_{42}$ for 2 h. After incubation, the medium containing FITC-Aβ was removed, and the cells were washed three times with 1xPBS. BV2 cells were collected by centrifugation at 3000rpm for 5min, and resuspended in ice-cold 1xPBS solution. The phagocytosed $A\beta_{42}$ content in BV2 cells was analyzed by flow cytometry, and PBS solution (PH4.4) was added to the sample for 1 min incubation before flow cytometry analysis to quench the cell surface-bound $A\beta_{42}$. To observe the effect of Dectin-1 on the degradation of $A\beta_{42}$ by BV2 cells, extracellular FITC-Aβ was removed after the cells were incubated with FITC-Aβ for 2 h. Cells were cultured in the FITC-Aβ-free medium for another 24 hours. Collect the cells and detect the level of intracellular Aβ by flow cytometry.

Molecular docking

The crystal structure of murine dectin-1 and human amyloid beta-peptide (1-42) were downloaded from RCSB Protein Data Bank (http://www.rcsb.org/) and the PDB ID for murine dectin-1 was 2BPD[1] while 6SZF[2] was for human amyloid beta-peptide (1-42). Protein-protein docking in ClusPro[3] was used for molecular docking simulation of dectin-1 and amyloid beta-peptide. For protein docking, 6SZF is set as ligand and 2BPD as receptor. The ligand was rotated with 70,000 rotations, among which 1000 rotation/translation combinations that have the lowest score was chosen. Then, a greedy clustering of these 1000 ligand positions with a 9 Å C-alpha RMSD radius was performed to find the ligand positions with the most "neighbors" in 9 Å, i.e., cluster centers. The top ten cluster centers with most cluster members were then retrieved and inspected visually one by one. The most likely models of the complex are selected on the basis of cluster population. The intermolecular contacts from the most probable poses were further evaluated. The models of the complex and interface residues were analyzed using MOE[4]. Molecular graphics were generated by PyMOL. The summary of interactions between dectin-1 and amyloid beta-peptide is listed in Table S3.

Surface Plasmon Resonance (SPR) analysis

The potential binding of $A\beta_{42}$ to recombinant human Dectin-1 (rhDectin-1, Sino Biological lnc, 10215-HNCH) was measured using Biacore T200 Protein Interaction Assay system (GE Healthcare) with a CM7 sensor chip (29-1470-20). Fifty μg rhDectin-1 protein was dissolved in 50 μL PBS Buffer (pH 7.4), and then amine coupling kit (Fortebio) was used to immobilize rhDectin-1 on the chip. Different doses of $A\beta_{42}$, including 62.5, 31.25, 15.625, 7.8, 3.4, 1.7, 0.85 μM were prepared with running buffer (PBS containing 0.02%Tween20). The sample plates and sensor were placed in the instrument. During the association phase, the interactions were determined at

a flow rate of 30 μL/min for 180 s, then the dissociation phase at 25°C for 250s. Data were analyzed using Biacore T200 manager software. The binding kinetic parameters were calculated by global fitting of the kinetic data from various concentrations of $A\beta_{42}$ using a 1:1 Langmuir binding model.

RNA-seq and bioinformatics analysis

RNA sequencing was performed by Wuhan *Huada Gene Technology Co., Ltd*. Two independently prepared *RNA* samples from each group *were* prepared for *RNA-Seq*. The sequencing data was filtered with SOAPnuke (v1.5.2). The clean reads were mapped to the reference genome using HISAT2 (v2.0.4). Then, Ericscript (v0.5.5) and rMATS (V3.2.5) were used to analyze the fused genes and differential splicing genes (DSGs), respectively. Bowtie2 (v2.2.5) was used to align the clean reads to the gene set, a database for this organism built by BGI (Beijing Genomic Institute in Shenzhen), which included known and novel coding transcripts. Gene expression levels were calculated using RSEM (V1.2.12). The heatmap was drawn by pheatmap (v1.0.8) according to the gene expression in different samples. The DESeq2 (v1.4.5) with Q value ≤ 0.05 was used for differential expression analysis. The sources of software were summarized in Table S4.

GEO Database Analysis

The Gene Expression Omnibus (GEO, http://www.ncbi.nlm.nih.gov/geo) contains the original data of many diseases for users to download and research. In the present study, gene expression profile datasets GSE173955 were obtained by searching GEO database in normal people and AD patients. The *Clec7a* mRNA expressions between brain tissue of AD patients (N=8) and non-AD patients (N=10) were analyzed.

Pull-down Assay

100μL of 20 μM biotinylated- $A\beta_{42}$ was added to streptavidin-agarose beads (50 μL) and incubated for 45 min at 4°C with biotin alone as a control. Lysates prepared from microglia cells and mouse brain tissues were then added to the streptavidin-agarose beads with biotinylated- $A\beta_{42}$. The mixture was incubated for 24h at 4°C under gentle rocking. Samples were then spun and washed 3 times. Then, 5x loading buffer was added in the elution buffer and boiled for 10min, and the samples were used for western blot analysis. Total lysates were used as an input control.

Real-time qPCR

Total RNA was isolated from cultured BV2 cells and brain tissues using TRIzol reagent (Thermo Fisher, 15596026) by standard techniques. Total RNA concentration was measured by a spectrophotometer. Then, PrimeScript RT-reagent Kit (Takara, RR037A) was used for cDNA synthesis. Real-time PCR amplification reactions were carried out on CFX96 Touch Real-Time PCR Detection System (Bio-Rad) using TB Green Premix Ex Taq II (Takara; RR820A). Quantification of the mRNA expression was calculated by $2^{\Delta\Delta Ct}$ method with *GAPDH* normalization. Primer sequences used in this study were presented in Supplementary Table S2.

Western blot analysis

The cultured BV2 cells or brain tissue samples under different treatments were lysed in ice-cold RIPA lysis buffer (P0013B; Beyotime Biological Technology, Shanghai, China) supplemented with a protease phosphatase inhibitor cocktail and the protein concentration was tested using a BCA protein assay kit. Samples with the same concentration of proteins were loaded on 12% SDS-PAGE gels, then transferred to 0.22 μm PVDF membrane at 300 mA for 2h. The PVDF membranes containing protein bands were blocked with 3% BSA for 1 h at room temperature and incubated with selective primary antibodies (1:1000) overnight at 4 °C. Following day, the primary antibody was washed with 1×TBST (Tris-buffered saline containing 0.05% Tween20) thrice, and incubated with horseradish peroxidase (HRP)-conjugated secondary antibody for another 2h at room temperature. After exposure with BCL, the intensity of bands were quantified using Image J software.

Statistical analysis

Data analysis was performed using GraphPad Prism 8.0 statistical software (GraphPad software, Inc., San Diego, CA, USA). Each experiment was carried out in triplicates and all the data was expressed as mean ± SEM. The statistical differences between multiple groups was determined using one or two-way ANOVA followed by Tukey's post-hoc test ($\alpha = 0.05$) to assess the difference between any two groups. For the MWM test, escape latency times in the hidden platform trial were analyzed via two-way ANOVA of repeated measures.

Results

Dectin-1 is up-regulated in AD model mice

In recent years, substantial evidence has shown that Dectin-1 is involved in neurological pathology [24]. Through GEO database analysis, we observed that the Dectin-1 mRNA level (CLEC7a) was significantly elevated in patients with AD compared to patients without AD (Figure S1). We further analyzed gene expression changes in the hippocampus of

mice with or without $A\beta_{42}$ injection using RNA Sequencing (RNA-seq) (Figure 1A). In this study, we used aggregated $A\beta_{42}$, as aggregated Aβ is more toxic. First, $A\beta_{42}$ was prepared as a 10 mM stock solution in sterile DMSO, then incubated at 37°C for 7 days before use. The aggregation state of $A\beta_{42}$ in this experiment was detected by non-denaturing gel and Coomassie brilliant blue staining. Obtained result showed that $A\beta_{42}$ after 37°C aggregation is a low molecular weight (LMW) oligomer (Figure S2). Immunofluorescence staining of APP/β-amyloid and the microglia marker Iba1 in the mouse hippocampus confirmed that $A\beta_{42}$ infusion successfully induced AD pathology (Figure S3A). Similar results were obtained in the western blot assay (Figure S3B). The data also showed that $A\beta_{42}$ injection increased the levels of the inflammatory factors tumor necrosis factor-α (TNFα) and IL-1β in the hippocampal tissue (Figure S3C). Interestingly, RNA-seq analysis showed that Dectin-1 mRNA levels were also significantly increased in the hippocampal tissue of $A\beta_{42}$-infused mice compared to those in the WT group (Figure 1B). Western blot assay of mouse hippocampal tissues validated the increased Dectin-1 level following $A\beta_{42}$ challenge (Figure 1C). To further confirm this, we used 8-month-old APP/PS1 mice as another AD model. As shown in Figure 1D, Dectin-1 protein levels were also significantly increased in the hippocampal tissues of APP/PS1 mice compared to WT mice (Figure 1D).

Dectin-1 has been reported to be highly expressed by myeloid-lineage cells such as macrophages [25]. Therefore, we expected microglia to be the primary source of increased Dectin-1 in brain tissue. To confirm this, we double-labeled microglia markers (Iba1), astrocyte markers (GFAP), Neuron markers (NeuN) and Dectin-1 in $A\beta_{42}$ injection models, respectively. As shown in Figure 1E, there is almost no expression of Dectin-1 in neurons, a small amount of Dectin-1 expression in astrocytes, and the highest relative expression in microglia, suggesting that microglia are the main cell type expressing Dectin-1 in the hippocampus (Figure 1E-F). We then examined Dectin-1 expression in the PC12 and BV2 cell lines. As expected, Dectin-1 was expressed in BV2 cells, but not in PC12 cells (Figure 1G). Taken together, these results further validate that Dectin-1 is expressed in microglia and is significantly increased in $A\beta_{42}$ infusion and APP/PS1 mouse models, suggesting that Dectin-1 in microglia may play an important role in the pathology of AD.

Dectin-1 knockout alleviates cognitive impairment in $A\beta_{42}$ infusion mice

To assess the role of Dectin-1 in the development of AD, Dectin-1 knockout (D1KO) mice were used. We first verified that Dectin-1 was knocked out in the brain tissue of D1KO mice (Figure S4A-B). Both WT and DIKO mice were injected with or without $A\beta_{42}$ to develop the AD model or control groups, respectively (Figure S5A). The Morris water maze (MWM) and novel object recognition assay (NOR) were used to assess learning and memory abilities in four groups: WT (wild-type), $A\beta_{42}$ ($A\beta_{42}$ injection), D1KO (Dectin-$1^{-/-}$), and D1KO+$A\beta_{42}$. The movement trajectory of each group of mice was recorded using the Morris water maze test (Figure 2A). The average escape latency of mice injected with $A\beta_{42}$ was significantly increased. However, the average escape latency of D1KO mice was significantly lower than that of mice in the $A\beta_{42}$ infusion group (Figure 2B-2C). After removing the platform, mice in the D1KO group spent more time crossing the platform and stayed in the target quadrant compared to mice in the $A\beta_{42}$ group (Figure 2D-2E). In addition, there were no significant differences in swimming speed and total distance between the different groups of mice (Figure 2F-2G), excluding the potential influence of differences in exercise capacity on this experiment. These results suggest that Dectin-1 knockout significantly alleviates cognitive impairment induced by $A\beta_{42}$ infusion. We further verified our results using a novel object recognition assay. The representative curves are shown in Figure 2H. We recorded the number of novel object explorations (Figure 2I), total time spent exploring novel objects (Figure 2J), and total latency to touch novel objects (Figure 2K) of the mice in each group. The results showed that the exploration of novel objects increased in the D1KO group compared to that in the $A\beta_{42}$ infusion group. These data indicate that knockout of Dectin-1 significantly improves cognitive impairment in $A\beta_{42}$ infusion model mice.

Dectin-1 knockout improves neuropathology in $A\beta_{42}$ infusion mice

Damage to brain synaptic structure and functional plasticity is a major pathology of AD, resulting in a decline in the learning and memory abilities of patients with AD [26]. Therefore, we examined synaptic plasticity. IF staining of the mouse hippocampus showed a significant loss of synapses in the $A\beta_{42}$ infusion mice, while the number of neurite cytoskeleton microtubule-associated protein 2 (MAP2)-expressing cells in the D1KO+$A\beta_{42}$ group was significantly increased (Figure 3A-3B). Western blotting validated the change in the expression of MAP2 and postsynaptic density protein 95 (PSD95) (Figure 3C-3E). Synaptic plasticity is important for maintaining neuronal function and activity in the CNS [27]. We tested the number of neuronal cells in

the hippocampus using NeuN staining. As shown in Figure 3F-3G, Dectin-1 deficiency reduced the number of apoptotic neurons in the $A\beta_{42}$-infused mouse hippocampus.

Dectin-1 knockout alleviates $A\beta_{42}$-induced microglia activation and inflammatory response

To further investigate the molecular mechanisms underlying the functions of Dectin-1 in AD, we isolated mRNA from all three groups of mice (WT, $A\beta_{42}$ and D1KO+ $A\beta_{42}$) and performed RNA-seq analysis. A total of 589 genes were identified (Figure 4A). Notably, microglial D1KO restored the levels of most of the upregulated genes and increased the levels of many of the downregulated genes (Figure 4B). To further characterize the inflammatory changes, we analyzed the levels of microglial markers, innate immune signaling genes, and inflammatory cytokines. As shown in Figure 4C, Dectin-1 knockout

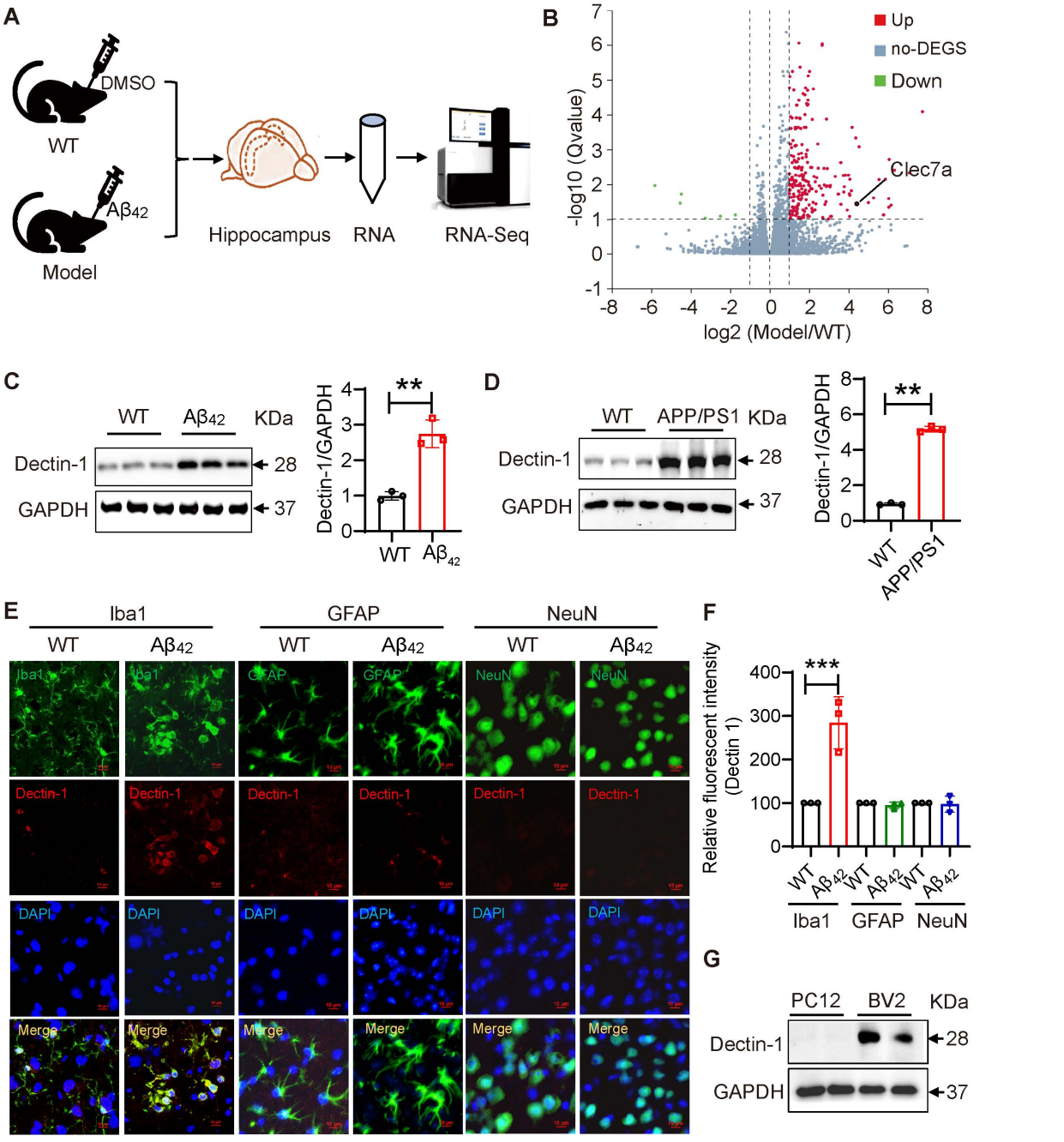

Figure 1: Dectin-1 is up-regulated in AD model mice. (A) RNA-seq analyses using hippocampus from the brains of C57 following DMSO infusion or C57 following $A\beta_{42}$ infusion for two weeks. N=6, 3 mice per group. **(B)** Bioinformatic analysis of RNA-seq. **(C)** Protein levels of Dectin-1 in the hippocampal tissue following $A\beta_{42}$ infusion. **(D)** Protein levels of Dectin-1 in the hippocampal tissues of APP/PS1 mice. **(E)** Representative dual-immunofluorescence staining of Microglia marker Iba1 (green), Astrocyte marker GFAP (green), Neuron Marker (NeuN) and Dectin-1 (red) in the hippocampal tissue of $A\beta_{42}$ infused mice. Sections were counterstained with DAPI (blue) [scale bar = 10 μm]. **(F)** Quantification analysis of Dectin-1 in E. **(G)** Western blot level of Dectin-1 in mouse bone marrow-derived macrophages (PC12), microglia cell line (BV2).

significantly reduced the increase in microglial markers (Itgam, Itgax, and C1qa), activated microglia markers (Cst7, Cxcl10, and CD68), NF-κB signaling genes (Rel1, Rel2, Nfkb1, Nfkb2, and Syk), and cytokines (Il1b, Tnfa, Il1a, and Il12b), suggesting inhibition of microglial activation and inflammatory activation. Similarly, Dectin-1 knockout significantly reduced the number of Iba1-positive cells (Figure 4D and 4G). We also tested the effect of Dectin-1 on the inflammatory response and NF-κB p65 using immunofluorescence staining (Figure 4E-4F and 4H-4J), western blotting (Figure 4K-4N) and ELISA (Fig S5A-5B). The data showed that injection of $A\beta_{42}$ resulted in increased release of the pro-inflammatory cytokines TNFα and IL–1β in mouse hippocampal tissues, while Dectin-1 deficiency blocked these changes. We next explored whether the canonical downstream Syk-NF-κB pathway of Dectin-1 [12] was activated by $A\beta_{42}$ injection. Hippocampal tissues from WT mice injected with $A\beta_{42}$ showed increased p-Syk, phosphorylated NF-κB p65, and nuclear NF-κB p65 translocation, indicating activation of Syk/NF-κB by $A\beta_{42}$ infusion (Figure 4O-4Q). Dectin-1 knockout mice reduced $A\beta_{42}$-induced Syk/NF-κB activation.

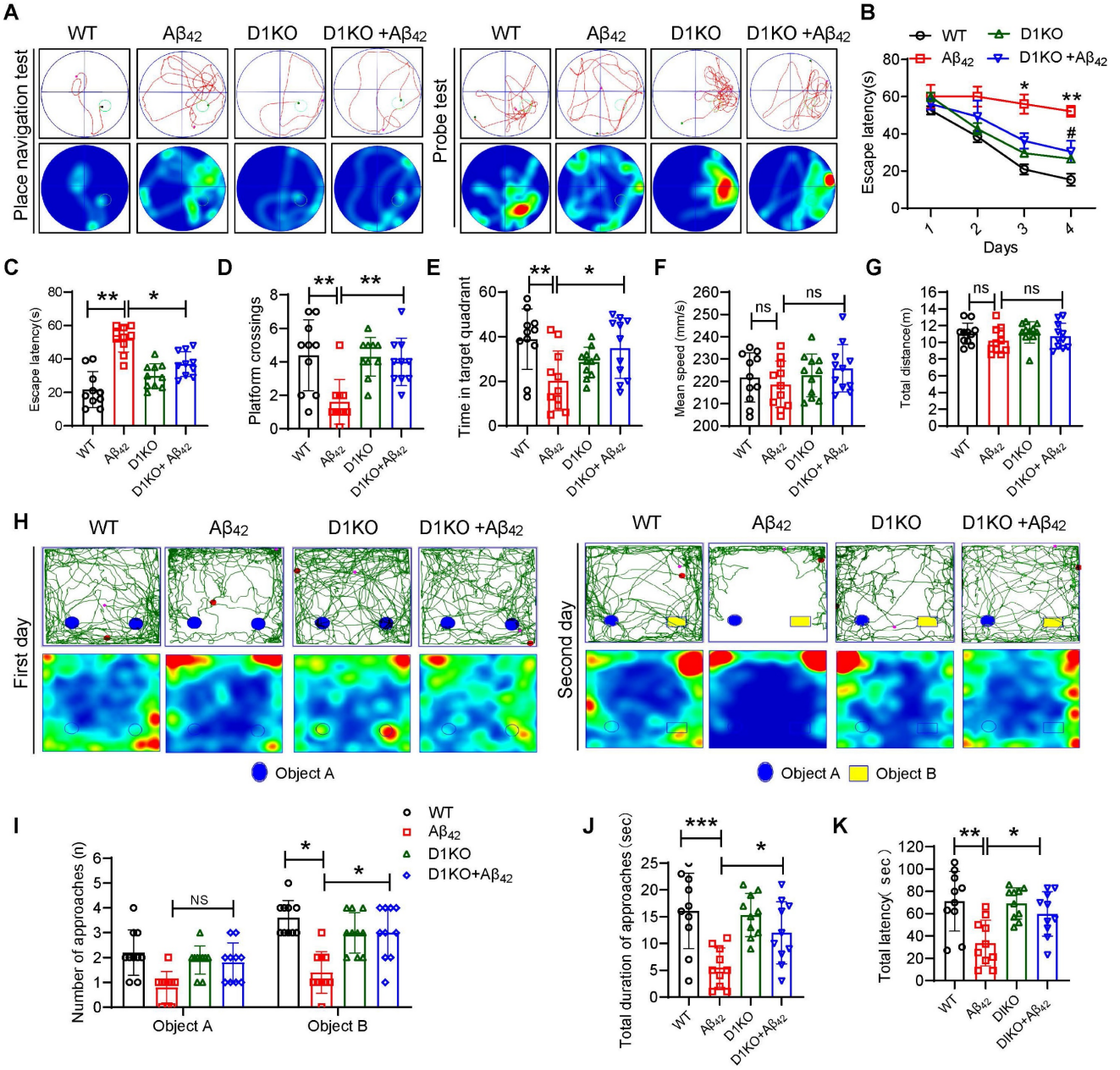

Figure 2: Dectin-1 knockout restore cognitive functions of $A\beta_{42}$ infusion model mice. (A) Representative average escape latency curves during place navigation test (four trials per day, during four consecutive days) and probe tests on day 5 without platform. N=40, N=10 mice per group. **(B)** Time course of escape latency, defined as the time taken to find the hidden platform. **(C)** Escape latency of all four groups on day 4. **(D)** The number of platform crossings. **(E)** The time in target quadrant. **(F)** Average swimming speed of mice in each group. **(G)** Total swimming distance of mice in each group. **(H)** Representative curves during novel object recognition test in each group. **(I)** Number of approaches in each group. **(J)** Total during of approaches in each group. **(K)** Total latency of all four groups.

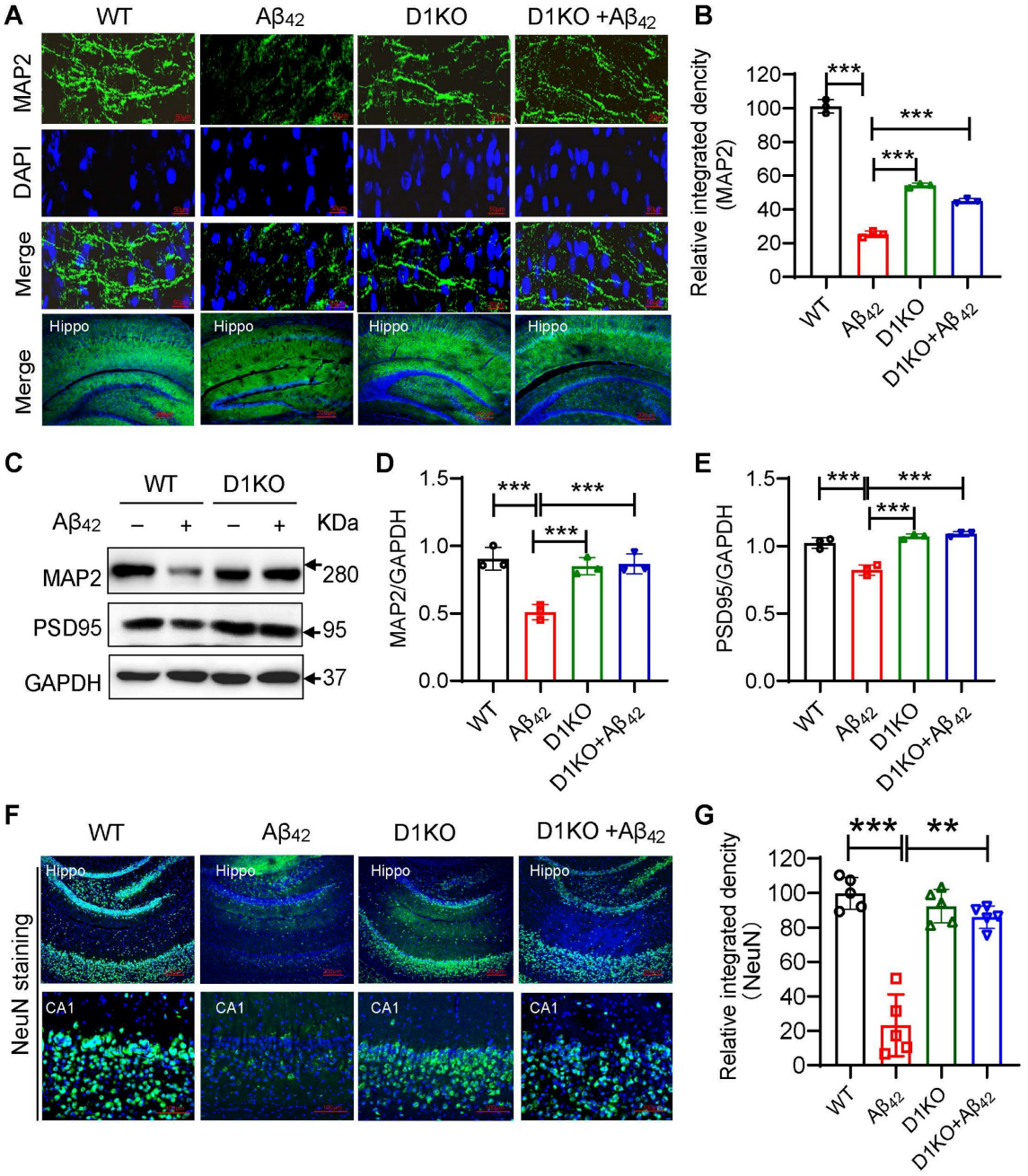

Figure 3: Dectin-1 knockout improves neuropathology of Aβ42 infusion mice. (A) Representative immunofluorescence staining of MAP2 (green) in brain tissues of WT and Aβ42 infusion mice. Sections were counterstained with DAPI (blue) [scale bar = 50 μm]. **(B)** Quantification of MAP2 staining. **(C)**Representative western blot analysis of MAP2 and PSD95 in hippocampal tissue lysates from WT and Aβ42 infusion mice. **(D)** Quantification and statistical analysis of MAP2 in C. **(E)** Quantification and statistical analysis of PSD95 in C. **(F)** IF of NeuN staining: Hippo [scale bar = 200 μm], CA1[scale bar = 100 μm] in brain tissues of WT and Aβ42 infusion mice. **(G)** Quantification of NeuN staining.

The anti-inflammatory actions of Dectin-1 deletion may result from two possible mechanisms: 1) Dectin-1 mediates the pro-inflammatory signaling pathway of Aβ and 2) Dectin-1 deletion reduces Aβ levels by promoting Aβ clearance in the hippocampus. Therefore, we measured the effect of Dectin-1 on Aβ clearance in the hippocampus. As shown in Figure S6B-6D, Dectin-1 deficiency did not affect the level of Aβ plaques in the mouse hippocampus. To verify the effect of Dectin-1 on phagocytosis and clearance of $Aβ_{42}$, we linked $Aβ_{42}$ with a FITC label (FITC-$Aβ_{42}$). We treated Dectin-1-deficient BV2 cells with FITC-Aβ for an appropriate time, and then used flow cytometry to detect the phagocytosis and clearance of $Aβ_{42}$ by Dectin-1. The obtained results found that the Dectin-1 deficiency did not affect the fluorescence intensity of Aβ (Fig S6E-6F), indicating that Dectin-1 does not mediate Aβ phagocytosis and clearance in microglia. Taken together, $Aβ_{42}$ activates Dectin-1 to induce Syk

phosphorylation and NF-κB activation, resulting in an increase in the levels of pro-inflammatory factors, rather than Aβ phagocytosis and clearance in microglia.

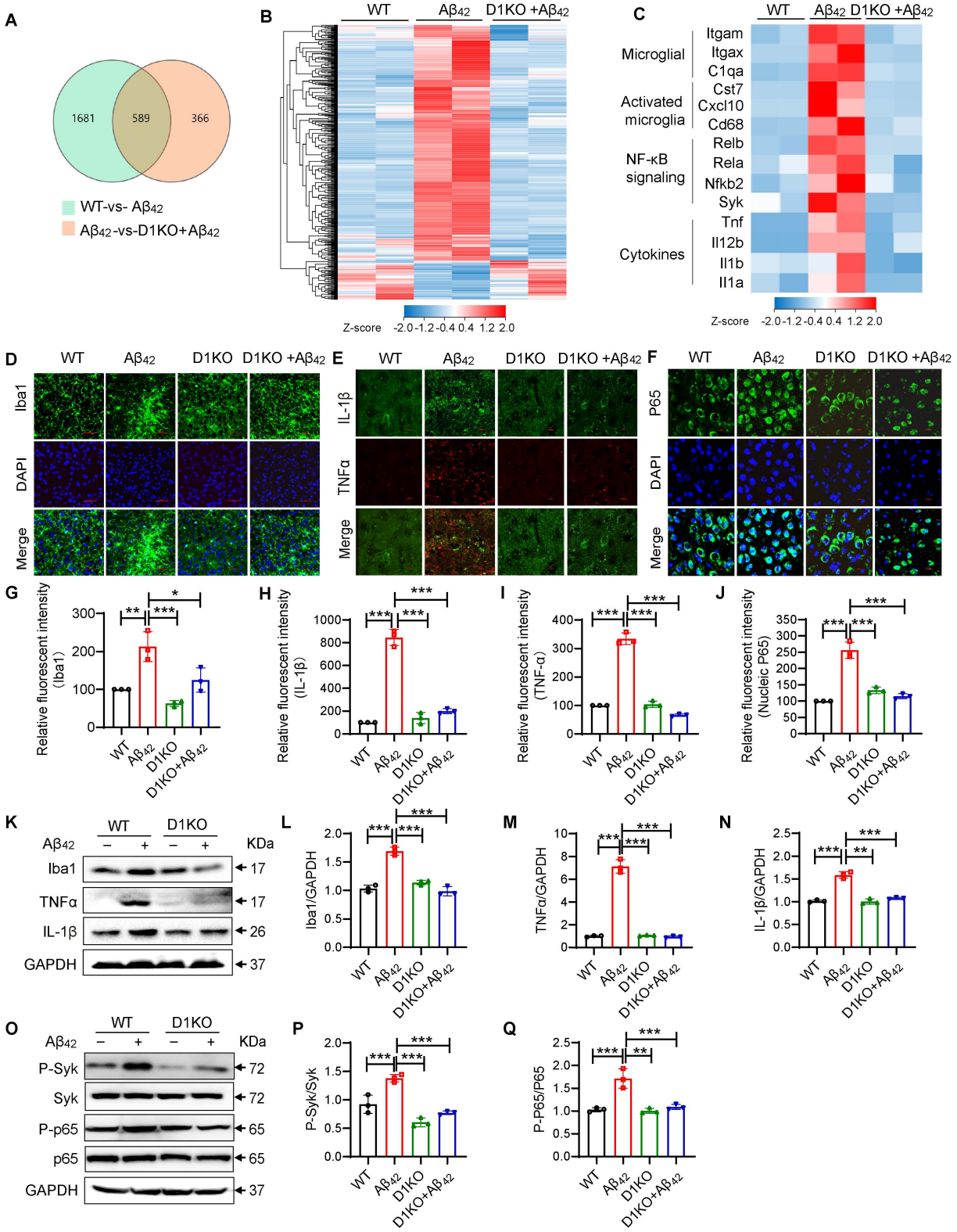

Figure 4: Dectin-1 mediates microglia activation and inflammatory response in brain tissue. (A) Venn diagram depicting expressed genes in WT-vs- Aβ42 and D1KO-vs- Aβ42. **(B)** Heatmap shows four groups of expressed genes that expressed differentially between 8-week-old WT, Aβ42, D1KO, and D1KO+ Aβ42 mice ($P < 0.05$). **(C)** Heatmap of microglia markers, markers in activated microglia, NF-κB signaling, and cytokines from these four groups of mice. **(D)** Representative immunofluorescence staining of Iba1(green) in brain tissues of WT and Model (Aβ42 infusion) mice. Sections were counterstained with DAPI (blue) [scale bar = 50 μm]. **(E)** Representative double-immunofluorescence staining of TNFα (red) and IL-1β (green). Slides were counterstained with DAPI (blue) [scale bar = 10 μm]. **(F)** Representative immunofluorescence staining of NFκB (green) in brain tissues of WT and Aβ42 infusion mice. Sections were counterstained with DAPI (blue) [scale bar = 10 μm]. **(G)** Quantification of Iba1 staining

in D. **(H-I)** Quantification of IL-1β and TNFα staining in E. **(J)** Quantification of NFκB staining in F. **(K-N)** Representative western blot analysis of Iba1, TNFα, and IL-1β in hippocampus tissue lysates. **(O-Q)** Representative western blot analysis of p-Syk, Syk, P-NFκB65, and NFκB65 in mouse brain tissue lysates.

$A\beta_{42}$ activates the Dectin-1-Syk signaling pathway by binding to Dectin-1 and inducing its homodimerization

Based on the apparent functional role of Dectin-1 in AD inflammation, we explored the potential molecular mechanisms underlying Dectin-1 activation by $A\beta_{42}$. Dectin-1 homodimerization and Syk recruitment are the two hallmarks of Dectin-1 activation. We first tested the interaction between Dectin-1 and Syk in microglia and in $A\beta_{42}$-infused mice. The results showed that $A\beta_{42}$ increased the interaction between Dectin-1 and Syk in a time-dependent manner in BV2 cells (Figure 5A). Increased Dectin-1-Syk interaction was also observed in the hippocampi of $A\beta_{42}$-infused mice (Figure S7A). Next, we transfected HEK-293 cells with Flag- and HA-tagged Dectin-1 and exposed the cells to $A\beta_{42}$. Co-IP analysis showed $A\beta_{42}$-induced Flag-HA interaction, indicating Dectin-1 homodimerization (Figure 5B). We also exposed microglia to 20 μM $A\beta_{42}$ for different durations to examine Syk phosphorylation and observed $A\beta_{42}$-induced Syk phosphorylation peaking at 45 min (Figure 5C). Furthermore, $A\beta_{42}$ challenge for 45 min induced Syk phosphorylation in a dose-dependent manner in BV2 cells (Figure 5D).

We then measured whether Dectin-1 mediated the $A\beta_{42}$-induced inflammatory response in cultured microglial BV2 cells. We interfered with Dectin-1 expression with siRNA targeting the Dectin-1 gene (siD1) in BV2 cells and verified the knockdown efficiency by western blotting (Figure 5E). Similarly, we found that $A\beta_{42}$ induced the Syk phosphorylation and NF-κB activation in BV2 cells, while this increased activity of Syk/NF-κB was not seen in Dectin-1-deficient BV2 cells (Figure 5E-5F). As shown in Figure 5G, knocking down Dectin-1 remarkably inhibited $A\beta_{42}$-induced p65 nuclear translocation in BV2 cells. These results are consistent with the effect of Dectin-1 in $A\beta_{42}$ infusion model mice. Assessment of neuroinflammation showed that Dectin-1 deficiency decreased the release of the inflammatory factors TNF-α and IL-1β (Figure 5H-5I). Moreover, the $A\beta_{42}$-increased mRNA levels of the inflammatory genes *Tnfa, Il1b, IL-6, Cox2,* and *Inos* were significantly reversed by siD1 in BV2 cells (Figure 5J).

$A\beta_{42}$ directly bind to Dectin-1

The triggering receptor expressed on myeloid cells 2 (Trem2) is a microglial surface receptor genetically linked to the risk of AD [28]. Most Aβ functions in microglia are thought to be mediated by its binding to Trem2 [29]. To better understand how $A\beta_{42}$ activates Dectin-1, we visualized the molecular processes using biotinylated $A\beta_{42}$ (Bio-$A\beta_{42}$). Bio-$A\beta_{42}$ retained the Dectin-1 activating activity of $A\beta_{42}$, as evidenced by the increased phosphorylation of Syk in microglia exposed to Bio-$A\beta_{42}$ (Figure S7B). After exposure of microglia to Bio-$A\beta_{42}$ or biotin, we performed immunofluorescence co-staining for Bio-$A\beta_{42}$, Dectin-1, and Trem2 and found that all of them were mainly located in the cell membrane. Trem2 is the currently reported microglia receptor that can directly bind to Aβ, and we used it as a positive control in this experiment. Interestingly, in addition to co-localization with Trem2, $A\beta_{42}$ also co-localized with Dectin-1 significantly on the cell surface (Figure 6A), indicating a potential interaction between $A\beta_{42}$ and Dectin-1. Co-IP analysis further confirmed this result (Figure 6B). Next, we performed a protein interaction analysis using Co-IP. APP/β-amyloid was added to Protein A magnetic beads as a bait protein, and lysates from WT and $A\beta_{42}$ brain tissues were added. Our results showed that APP/β-amyloid binds to the Dectin-1 protein in these lysates. In turn, we could also capture the expression of APP/β-amyloid protein using Dectin-1 as a bait protein (Figure 6C). The above data prompted us to hypothesize that $A\beta_{42}$ may act as a ligand and directly interact with Dectin-1 in the microglia. Therefore, we used surface plasmon resonance (SPR) to identify direct $A\beta_{42}$-Dectin-1 interactions at the molecular level. As shown in Figure 6D, $A\beta_{42}$ interacted with recombinant human Dectin-1 (rhDectin-1) protein with high affinity.

To strengthen this finding, we conducted molecular docking to analyze the interaction between Dectin-1 and amyloid beta peptide. The weighted energy score of the cluster center of complex Dectin-1 and amyloid beta peptide is -820.5 kcal/mol and the energy score of the lowest energy structure in the cluster is -908.1 kcal/mol. The interaction between Dectin-1 and amyloid beta peptide is depicted in Figure 6E. A summary of the interactions between Dectin-1 and amyloid beta peptide is presented in Table S3. The surface binding model of Dectin-1 and amyloid beta peptide is shown in Figure S8A-C. The Dectin-1 is colored in cyan, whereas amyloid beta peptide is colored in wheat. These interactions mainly contribute to the binding energy between Dectin-1 and amyloid beta peptide. Taken together, these results show that Dectin-1 can directly bind to $A\beta_{42}$.

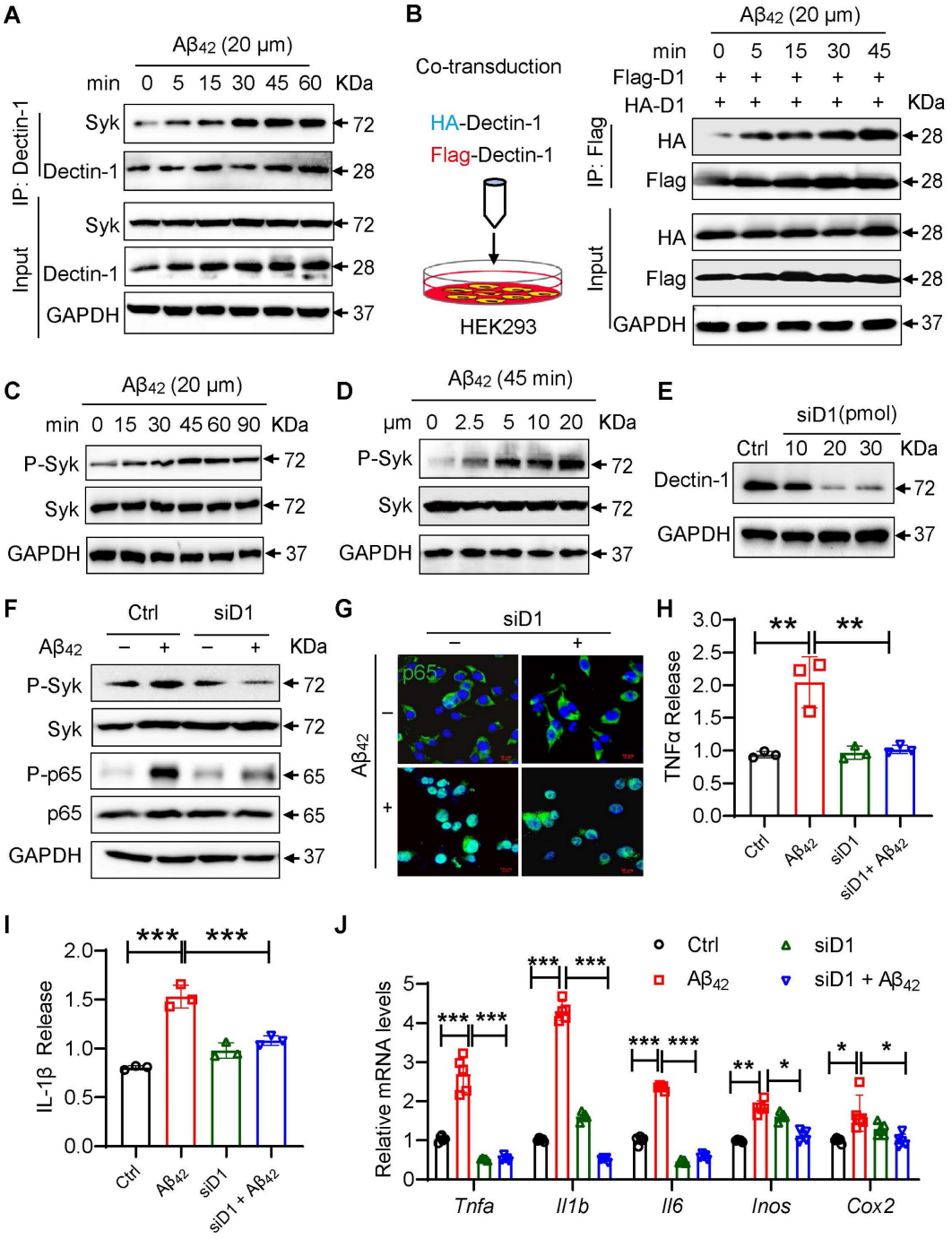

Figure 5: Dectin-1 interference prevents Aβ42-induced inflammatory response in BV2 cells. (A) Time-course of Dectin-1-Syk interaction. BV2 cells were exposed to 20 μM Aβ42 for indicated times and co-immunoprecipitation using Dectin-1 antibody to probe for Syk was performed. **(B)** HEK-293T cells were transfected with Flag-tagged Dectin-1 (Flag-D1) and HA-tagged Dectin-1 (HA-D1). Time-course of Dectin-1 dimerization (Flag-HA interaction) assessed following exposure of cell to 20 μM Aβ42 for indicated times. **(C)** Time-course of Syk phosphorylation. BV2 cells are exposed to 20 μM Aβ42 for indicated times. Total proteins were extracted and probed for p-Syk and Syk levels. GAPDH was used as loading control. **(D)** Dose-course of Syk phosphorylation. BV2 cells were exposed to increasing levels of Aβ42 for 45 mins. Total proteins were used to measure p-Syk and Syk levels. GAPDH was used as loading control. **(E)** Determination of Dectin-1 interference efficiency in BV2 cells. Total proteins were extracted and probed for p-Syk and Syk levels. GAPDH was used as loading control. **(F)** Representative western blot analysis of p-Syk, Syk, P-NFκB65, and NFκB65 in BV2 cells. GAPDH was used as loading control. **(G)** Representative immunofluorescence staining of NFκB65 (green) in BV2 cells transfected with or without siD1 [scale bar = 10 μm]. **(H)** TNFα release in cell supernatant measured by ELISA. **(I)** IL-1β release in in cell supernatant measured by ELISA. **(J)** mRNA levels of *Tnfa, Il1b, Il6, Inos,* and *Cox2* in the hippocampus tissues. Transcript levels were normalized to *GAPDH*.

Dectin-1 deficiency in microglia ameliorates Aβ42-induced neuronal cell damage

The activation of microglia and inflammation-mediated neurotoxicity have been suggested to play key roles in the pathogenesis of AD [30]. To assess the effect of macroglia-derived inflammatory factors on neuronal cells, we prepared conditioned media from BV2 cells. BV2 cells with or without siD1 pretreatment were exposed to Aβ42 for 6 hours, washed with 1xPBS,

and then replaced with 10% DMEM medium for 24 hours to collect conditioned medium. PC12 cells were treated with microglia-conditioned medium for 24 h to detect the damaging effect of the inflammatory environment on neuronal cells (Figure 7A). The results showed that conditioned media from microglia exposed to $A\beta_{42}$ increased PC12 apoptosis and intracellular ROS production (Figure 7B-7G). Media produced from Dectin-1-deficient microglia failed to damage PC12 cells. Collectively, these results demonstrated that blocking Dectin-1 in microglia suppressed $A\beta_{42}$-induced inflammatory mediators and subsequent intercellular crosstalk, resulting in reduced neuronal cell damage.

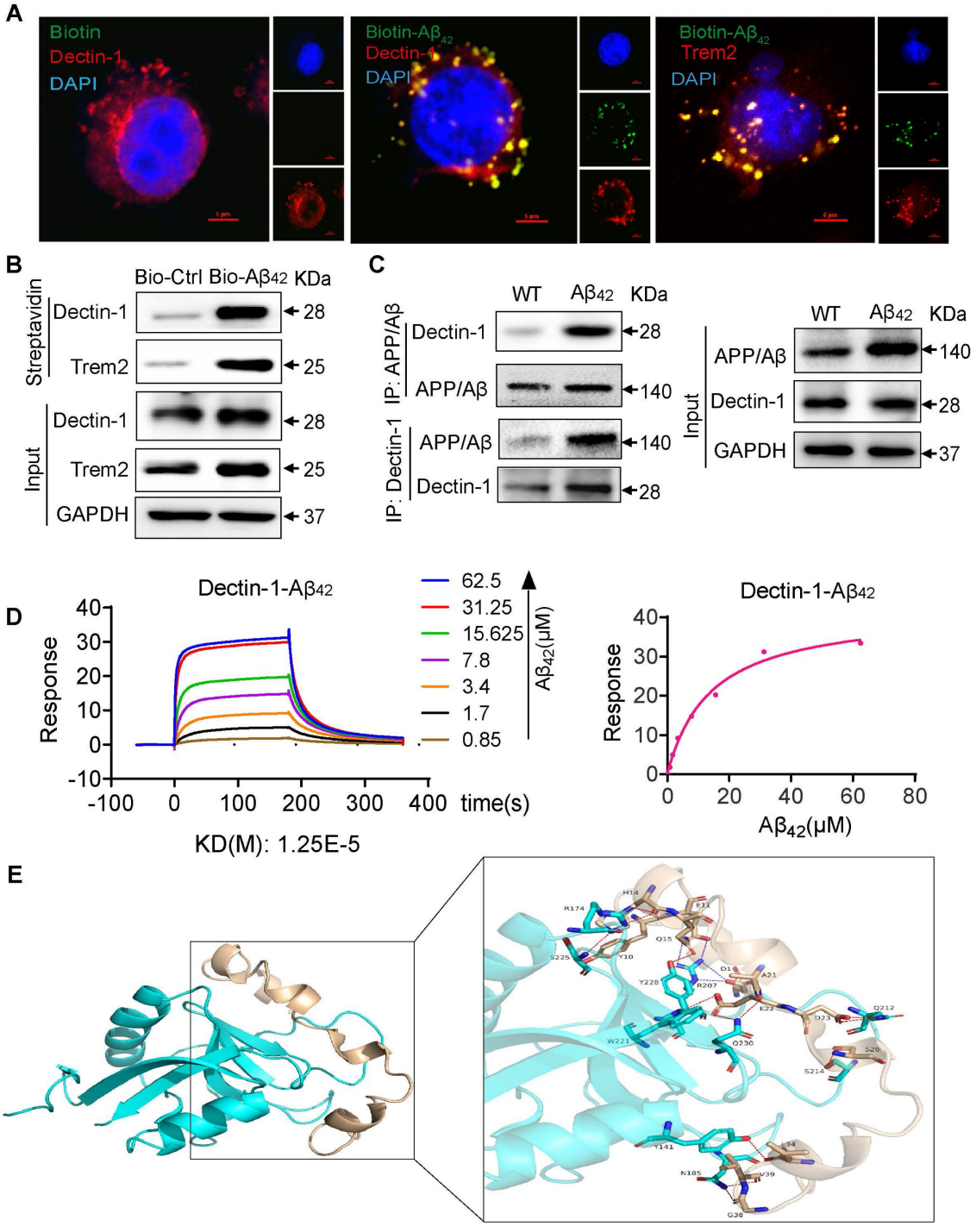

Figure 6: $A\beta_{42}$ activates the Dectin-1-Syk signaling pathway by binding to Dectin-1 and inducing its homodimerization. (A) BV2 cells are treated with 20 μM Bio- $A\beta_{42}$ or free biotin for 45 min, and cells are double-stained for biotin (green) and Dectin-1 (red) or Trem 2 (red), respectively. Nuclei are counterstained with DAPI (blue) [scale bar = 5 μm]. **(B)** Bio-$A\beta_{42}$ is added to streptavidin-agarose beads and incubated. Biotin alone was used as control. Lysates prepared from BV2 cells were added to beads. The eluent was loaded onto a polyacrylamide gel for western blot analysis. Total lysates were used as input controls. Trem2 was used as a positive control. **(C)** The Dectin-1-APP/ β-amyloid interaction is analyzed by co-immunoprecipitation in the brains of WT and model mice. **(D)** Surface plasmon resonance (SPR) analysis showing a direct interaction between $A\beta_{42}$ and rhDectin-1. Mean KD constant derived from five separate experiments. **(E)** 3D binding model of dectin-1 and amyloid beta peptide. The backbones

of dectin-1 and amyloid beta peptide are shown as cartoons. The residues in dectin-1 are shown as cyan sticks, whereas the residues in amyloid beta-peptide are shown as wheat sticks. The hydrogen bonds are depicted as red dashed lines and the salt bridges are depicted as blue dashed lines.

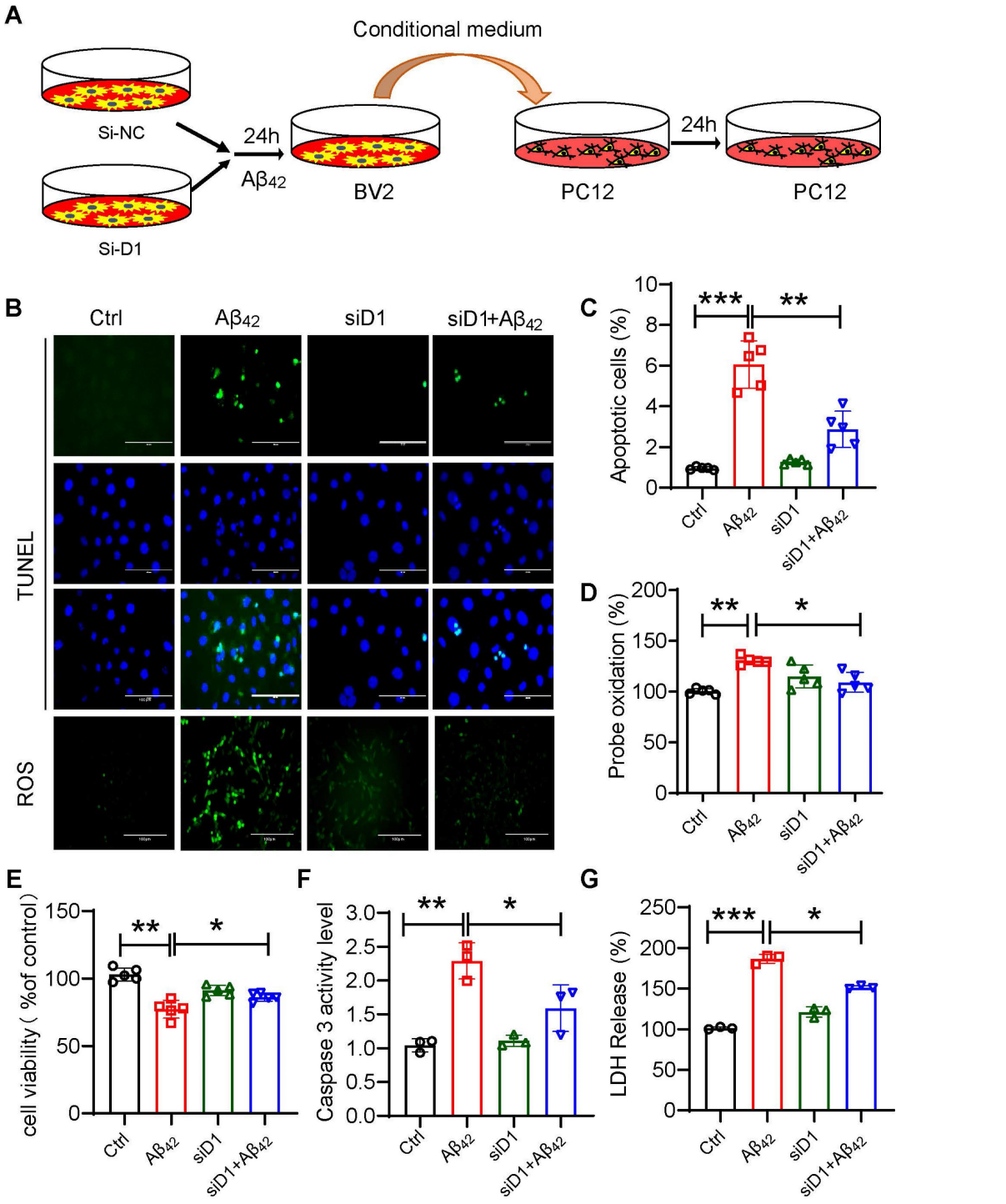

Figure 7: Dectin-1 interference prevents Aβ42-induced neuronal damage. (A) BV2 cells pretreated with siD1 for 24 h are stimulated with/without 20 μM Aβ42 for another 24 h, and the conditioned culture supernatant is collected. **(B)** PC12 cells are plated into four groups: CTL, Aβ42, siD1, and siD1+Aβ42; BV2 serum is added to stimulate the PC12 cells for 24 h; and cell viability is measured by MTT assay. **(C)** LDH assay is used to test cell membrane damage. **(D)** TUNEL staining and Ros staining are used to test the apoptosis and intracellular ROS level [scale bar = 100 μm]. **(E)** Quantification of apoptotic cell in TUNEL staining in C. **(F)** Caspase 3 activity is detected using caspase 3 assay. **(G)** Quantification of ROS staining in D.

Discussion

In this study, we discovered an important role of microglial Dectin-1 in mediating Aβ-induced neuroinflammation and AD pathology. We found that microglial Dectin-1 levels were increased in AD models. Knockout of Dectin-1 ameliorated cognitive impairment and neuronal cell death in Aβ42 infusion model mice by inhibiting Aβ42-induced microglial activation and inflammatory cytokine release.

Mechanically, our studies showed that $A\beta_{42}$ binds directly to the extracellular domain of Dectin-1 to activate the Dectin-1-Syk-NF-κB pro-inflammatory signaling pathway in microglia. Taken together, these studies have identified a new $A\beta_{42}$ receptor in inflammatory induction and AD pathology.

Studies have shown that microglia play an important role in the development of AD [31]. Microglia act as "macrophages" in the brain, which are very sensitive to brain damage [32]. In the brains of AD models, β-amyloid plaques are surrounded by activated microglia [33]. In-depth research on the pathogenesis of AD has shown that neuroinflammation is an important mediator of Aβ-induced neuronal death and is an important factor in AD pathology [34],[35]. Studies have shown that Aβ can induce a significant increase in the expression of the inflammatory cytokines TNF-α and IL-6. In the early stages of AD, the inflammatory cytokine gene-related transcription factor NF-κB can be activated by Aβ deposition [36]. Several studies have revealed that Aβ stimulates pro-inflammatory activation of primary microglia [37, 38]. Hong et al. have demonstrated that microglia engulf abnormal synapses when challenged with oligomeric Aβ [39]. In this study, we analyzed neuroinflammation in the brain following $A\beta_{42}$ infusion. Experimental animal models of AD can be generated by stereotaxic injection of $A\beta_{42}$ because it induces characteristic pathological changes of AD, such as Aβ deposition, neuroinflammation, and learning and memory dysfunction [40-42]. Therefore, $A\beta_{42}$-injected animals are one of the suitable experimental models to explore the treatment of AD to study the mechanism of toxicity against $A\beta_{42}$. As expected, we found elevated levels of pro-inflammatory factors and an increased number of microglia in $A\beta_{42}$ infusion model mice. An imbalance in the inflammatory environment can cause neuronal cell damage. These results are consistent with those of previous studies. However, little is known about the precise molecular mechanism by which $A\beta_{42}$ induces microglial inflammatory responses.

Dectin-1 was first identified as a PRR of β-glucans in fungal pathogens [43]. Interestingly, recent studies have shown that Dectin-1 is also involved in non-pathogen-mediated sterile inflammation in addition to the classical β-glucan ligand. Dectin-1 has been reported to ligate lectin galectin-9 to promote pancreatic carcinoma immune-tolerance [14]. Recently, studies have explored the biological role of Dectin-1 in brain-related diseases. Dectin-1 signaling plays a crucial role in inflammatory activation after ischemic stroke [44]. In addition, Dectin-1 limits autoimmune neuroinflammation and promotes myeloid cell-astrocyte crosstalk in encephalomyelitis (EAE) [45]. In the APP/PS1 mouse model of AD, Dectin-1 was upregulated by apolipoprotein E4 (APOE4) in the plaque microenvironment, suggesting that APOE4-regulated Dectin-1 expression may represent a risk protein for AD [46]. These studies suggest an important role of Dectin-1 in CNS diseases. Our study is the first to investigate the role of Dectin-1 in the pathogenesis of AD. We showed that microglia Dectin-1 is overexpressed in AD model mice and that $A\beta_{42}$ quickly activates Dectin-1 as well as its downstream signals to promote microglial activation and inflammation.

Trem2 is recognized as a cell surface receptor of Aβ in microglia [47]. Studies have found that Trem2 is upregulated near Aβ plaques in AD models and is thought to respond to Aβ [48]. Aβ directly binds to Trem2 and potently inhibits $A\beta_{42}$ polymerization [49]. There are many interventions targeting the Trem2 pathway as therapeutic targets for AD. However, Trem2 deficiency reduces amyloid pathology in the early stages of AD but aggravates its pathology in the late stage [50], so it is not suitable as a potential target for the treatment of AD. Dectin-1 has been reported to be highly expressed on various myeloid cells including monocyte/macrophage and neutrophil lineages [51]. Our study confirmed the colocalization of Dectin-1 protein with $A\beta_{42}$. We also found that Dectin-1 did not affect the clearance of $A\beta_{42}$ in microglia. These data indicate that Dectin-1 is a novel and non-classic receptor of $A\beta_{42}$ for $A\beta_{42}$-induced inflammation in microglia. Compared to Trem2, targeting Dectin-1 may provide a new and effective strategy for the AD therapy.

Studies have identified an important role of microglia-mediated neuroinflammation in the development of AD. Our in vitro study also showed that Dectin-1 deficiency in microglia significantly reduced PC12 cell injury induced $A\beta_{42}$-challenged microglia medium. As mentioned above, Dectin-1-mediated microglial inflammation subsequently damages the neuronal cells. We also found that Dectin-1 knockout has a comprehensive reversal effect on AD pathology, including cognitive function, synaptic plasticity, neuroinflammation, and neuronal cell injury, suggesting that Dectin-1 deficiency can be a therapeutic strategy for AD. However, some questions still need to be addressed. For example, does Dectin-1 in astrocytes and circulating macrophages also contribute to neuroinflammation and AD pathology in $A\beta_{42}$-induced mice? Although we showed that Dectin-1 is mainly expressed in microglia in $A\beta_{42}$-induced whole-body Dectin-1 KO mice. We acknowledge that microglia-specific Dectin-1 knockout may be more accurate. Therefore, a limitation of this study is that it was not performed using

microglia-specific Dectin-1 knockout mice. In addition, another question is, besides $A\beta_{42}$, whether other stimuli (or $A\beta_{42}$-produced DAMPs) can activate Dectin-1 in AD and promote the development of AD. This is an important direction worthy of future research and will extend our understanding of neuroinflammation in AD. Our *in vitro* results demonstrated that $A\beta_{42}$ could directly activate microglial Dectin-1, which supports the current conclusion of this work. Further studies are needed to illustrate the contribution of Dectin-1 to other cell types.

In conclusion, to our knowledge, this is the first study to identify Dectin-1 as a new $A\beta_{42}$ receptor in AD pathology. We demonstrated that microglia Dectin-1 mediates $A\beta_{42}$-induced Syk/NF-κB signaling pathway activation and inflammatory response and subsequently contributes to AD pathology and cognitive dysfunction. We provide evidence for the direct binding of $A\beta_{42}$ to Dectin-1 and a deep understanding of the pro-inflammatory mechanism of $A\beta_{42}$. This study suggests that Dectin-1 may represent an attractive new strategy for the treatment of AD.

Abbreviations

$A\beta_{42}$: Amyloid beta peptide 1-42; Bio-$A\beta_{42}$: biotin-labeled Amyloid beta peptide; D1KO: Dectin-1$^{-/-}$; siD1: siRNA targeting Dectin-1 gene; IL-1β: Interleukin 1 beta; IL-6: Interleukin-6; ITAM: immunoreceptor tyrosine-based activation motif; SPR: surface plasmon resonance; Syk: spleen tyrosine kinase TAC; TNFα: Tumor necrosis factor-α; WGA: wheat germ agglutinin; Iba1: Induction of brown adipocytes; Inos: inducible NOS; Cox2: Cytochrome c oxidase subunit 2; GAPDH: glyceraldehyde 3-phosphate dehydrogenase; CLEC7A: (C-Type Lectin Domain Containing 7A; PRRs: Pattern recognition receptors; MAP2: microtubule-associated protein 2; PSD95: postsynaptic density protein 95; TUNEL: Terminal-deoxynucleoitidyl Transferase Mediated Nick End Labeling; RIPA: Radio immunoprecipitation assay; SDS-PAGE: 67 Sodium dodecyl sulfate polyacrylamide gel electrophoresis.

Supplementary Material

Supplementary figures and tables.
https://www.ijbs.com/v19p3249s1.pdf

Acknowledgements

This study was supported by the National Natural Science Foundation of China (21961142009 to G.L.), Zhejiang Provincial Key Scientific Project (2021C03041 to G.L.), Natural Science Foundation of Zhejiang province (LQ23H090018 to X.Z.) and Hangzhou medical college (00004F1RCYJ2109 to X.Z.).

Author contributions

Guang Liang and Xia Zhao contributed to the literature search and study design. Guang Liang and Xia Zhao participated in the drafting of the article. Xia Zhao, Jinfeng Sun, Li Xiong, Lingyu She, Liwei Li, Xue Han, and Shiju Ye carried out the experiments. Fan Chen, Xu Wang and Wei Wang revised the manuscript. Hao Tang, Yuqing Zeng, Li Xiong and Shiju Ye contributed to data collection and analysis.

Competing Interests

The authors have declared that no competing interest exists.

References

1. Wei, Cao, Hui, Zheng. Peripheral immune system in aging and Alzheimer's disease. Molecular neurodegeneration. 2018.
2. Lloyd AF, Miron VE. The pro-remyelination properties of microglia in the central nervous system. Nat Rev Neurol. 2019; 15: 447-58.
3. Misra A, Chakrabarti SS, Gambhir IS. New genetic players in late-onset Alzheimer's disease: Findings of genome-wide association studies. Indian J Med Res. 2018; 148: 135-44.
4. Zhang, Can, Browne, Andrew, DiVito, Jason, et al. Amyloid-β Production Via Cleavage of Amyloid-β Protein Precursor is Modulated by Cell Density. Journal of Alzheimer's Disease. 2010.
5. Selkoe DJ, Hardy J. The amyloid hypothesis of Alzheimer's disease at 25years. Embo Mol Med. 2016; 8: 595-608.
6. Jekabsone A, Mander PK, Tickler A, Sharpe M, Brown GC. Fibrillar beta-amyloid peptide Abeta1-40 activates microglial proliferation via stimulating TNF-alpha release and H2O2 derived from NADPH oxidase: a cell culture study. J Neuroinflammation. 2006; 3: 24.
7. Kim HY, Kim HV, Jo S, Lee CJ, Choi SY, Kim DJ, et al. EPPS rescues hippocampus-dependent cognitive deficits in APP/PS1 mice by disaggregation of amyloid-beta oligomers and plaques (vol 6, 8997, 2015). Nature Communications. 2016; 7.
8. Shen TY, Poliacek I, Rose MJ, Musselwhite MN, Kotmanova Z, Martvon L, et al. The role of neuronal excitation and inhibition in the pre-Botzinger complex on the cough reflex in the cat. J Neurophysiol. 2022; 127: 267-78.
9. Keren-Shaul H, Spinrad A, Weiner A, Matcovitch-Natan O, Dvir-Szternfeld R, Ulland TK, et al. A Unique Microglia Type Associated with Restricting Development of Alzheimer's Disease. Cell. 2017; 169: 1276-90 e17.
10. Thompson MR, Kaminski JJ, Kurt-Jones EA, Fitzgerald KA. Pattern recognition receptors and the innate immune response to viral infection. Viruses. 2011; 3: 920-40.
11. Gringhuis SI, Kaptein TM, Wevers BA, Theelen B, van der Vlist M, Boekhout T, et al. Dectin-1 is an extracellular pathogen sensor for the induction and processing of IL-1 beta via a noncanonical caspase-8 inflammasome. Nature Immunology. 2012; 13: 246-U63.
12. Wheeler ML, Limon JJ, Underhill DM. Immunity to Commensal Fungi: Detente and Disease. Annual review of pathology. 2017; 12: 359-85.
13. Gringhuis SI, Kaptein TM, Wevers BA, Theelen B, van der Vlist M, Boekhout T, et al. Dectin-1 is an extracellular pathogen sensor for the induction and processing of IL-1β via a noncanonical caspase-8 inflammasome. Nature Immunology. 2012; 13: 246-54.
14. Daley D, Mani VR, Mohan N, Akkad N, Ochi A, Heindel DW, et al. Dectin 1 activation on macrophages by galectin 9 promotes pancreatic carcinoma and peritumoral immune tolerance. Nat Med. 2017; 23: 556-67.
15. Fu X, Zeng H, Zhao J, Zhou G, Zhou H, Zhuang J, et al. Inhibition of Dectin-1 Ameliorates Neuroinflammation by Regulating Microglia/Macrophage Phenotype After Intracerebral Hemorrhage in Mice. Transl Stroke Res. 2021; 12: 1018-34.
16. Fu X, Zeng H, Zhao J, Zhou G, Chen G. Correction to: Inhibition of Dectin-1 Ameliorates Neuroinflammation by Regulating Microglia/Macrophage Phenotype After Intracerebral Hemorrhage in Mice. Translational stroke research.
17. Ye XC, Hao Q, Ma WJ, Zhao QC, Cui GY. Dectin-1/Syk signaling triggers neuroinflammation after ischemic stroke in mice. 2019.
18. Reid DM, Montoya M, Taylor PR, Borrow P, Gordon S, Brown GD, et al. Expression of the beta-glucan receptor, Dectin-1, on murine leukocytes in situ correlates with its function in pathogen recognition and reveals potential roles in leukocyte interactions. J Leukoc Biol. 2004; 76: 86-94.
19. Facchinetti R, Bronzuoli MR, Scuderi C. An Animal Model of Alzheimer Disease Based on the Intrahippocampal Injection of Amyloid β-Peptide (1-42). Methods in molecular biology. 2018; 1727: 343-52.

20. Paxinos G, Franklin KBJ. The mouse brain in stereotaxic coordinates. Compact 2nd ed. Amsterdam ; Boston: Elsevier Academic Press; 2004.
21. Reiserer RS, Harrison FE, Syverud DC, McDonald MP. Impaired spatial learning in the APPSwe + PSEN1DeltaE9 bigenic mouse model of Alzheimer's disease. Genes Brain Behav. 2007; 6: 54-65.
22. Bromley-Brits K, Deng Y, Song W. Morris water maze test for learning and memory deficits in Alzheimer's disease model mice. Journal of visualized experiments : JoVE. 2011.
23. Vorhees CV, Williams MT. Morris water maze: procedures for assessing spatial and related forms of learning and memory. Nat Protoc. 2006; 1: 848-58.
24. Giron LB, Peluso MJ, Ding J, Kenny G, Zilberstein NF, Koshy J, et al. Markers of fungal translocation are elevated during post-acute sequelae of SARS-CoV-2 and induce NF-kappaB signaling. JCI Insight. 2022.
25. Goodridge HS, Reyes CN, Becker CA, Katsumoto TR, Ma J, Wolf AJ, et al. Activation of the innate immune receptor Dectin-1 upon formation of a 'phagocytic synapse'. Nature. 2011; 472: 471-5.
26. Skaper SD, Facci L, Zusso M, Giusti P. Synaptic Plasticity, Dementia and Alzheimer Disease. CNS Neurol Disord Drug Targets. 2017; 16: 220-33.
27. Martella G, Bonsi P, Johnson SW, Quartarone A. Synaptic Plasticity Changes: Hallmark for Neurological and Psychiatric Disorders. Neural Plast. 2018; 2018: 9230704.
28. Gussago C, Casati M, Ferri E, Arosio B. The Triggering Receptor Expressed on Myeloid Cells-2 (TREM-2) as Expression of the Relationship between Microglia and Alzheimer's Disease: A Novel Marker for a Promising Pathway to Explore. J Frailty Aging. 2019; 8: 54-6.
29. Zhong L, Wang Z, Wang D, Wang Z, Martens YA, Wu L, et al. Amyloid-beta modulates microglial responses by binding to the triggering receptor expressed on myeloid cells 2 (TREM2). Mol Neurodegener. 2018; 13: 15.
30. Venero JL, Burguillos MA, Brundin P, Joseph B. The executioners sing a new song: killer caspases activate microglia. Cell Death Differ. 2011; 18: 1679-91.
31. Cosker K, Mallach A, Limaye J, Piers TM, Staddon J, Neame SJ, et al. Microglial signalling pathway deficits associated with the patient derived R47H TREM2 variants linked to AD indicate inability to activate inflammasome. Sci Rep. 2021; 11: 13316.
32. Rock RB, Gekker G, Hu S, Sheng WS, Cheeran M, Lokensgard JR, et al. Role of microglia in central nervous system infections. Clinical microbiology reviews. 2004; 17: 942-64.
33. Akama KT, Van Eldik LJ. β-Amyloid stimulation of inducible nitric-oxide synthase in astrocytes is interleukin-1β-and tumor necrosis factor-α (TNFα)-dependent, and involves a TNFα receptor-associated factor-and NFκB-inducing kinase-dependent signaling mechanism. Journal of Biological Chemistry. 2000; 275: 7918-24.
34. Bicca MA, Costa R, Loch-Neckel G, Figueiredo CP, Medeiros R, Calixto JB. B(2) receptor blockage prevents Abeta-induced cognitive impairment by neuroinflammation inhibition. Behav Brain Res. 2015; 278: 482-91.
35. MERAZ RIOS MA, Toral-Rios D, Franco-Bocanegra D, Villeda-Hernández J, Campos-Peña V. Inflammatory process in Alzheimer's Disease. Frontiers in integrative neuroscience. 2013; 7: 59.
36. Balez R, Steiner N, Engel M, Muñoz SS, Lum JS, Wu Y, et al. Neuroprotective effects of apigenin against inflammation, neuronal excitability and apoptosis in an induced pluripotent stem cell model of Alzheimer's disease. Scientific reports. 2016; 6: 1-16.
37. Sondag CM, Dhawan G, Combs CK. Beta amyloid oligomers and fibrils stimulate differential activation of primary microglia. Journal of neuroinflammation. 2009; 6: 1-13.
38. Yao Y, Li J, Niu Y, Yu JQ, Yan L, Miao ZH, et al. Resveratrol inhibits oligomeric Aβ-induced microglial activation via NADPH oxidase. Molecular medicine reports. 2015; 12: 6133-9.
39. Hong S, Beja-Glasser VF, Nfonoyim BM, Frouin A, Li S, Ramakrishnan S, et al. Complement and microglia mediate early synapse loss in Alzheimer mouse models. Science. 2016; 352: 712-6.
40. Huo D-s, Sun J-f, Zhang B, Yan X-s, Wang H, Jia J-x, et al. Protective effects of testosterone on cognitive dysfunction in Alzheimer's disease model rats induced by oligomeric beta amyloid peptide 1-42. Journal of Toxicology and Environmental Health, Part A. 2016; 79: 856-63.
41. Zhao X, Huang X, Yang C, Jiang Y, Zhou W, Zheng W. Artemisinin Attenuates Amyloid-Induced Brain Inflammation and Memory Impairments by Modulating TLR4/NF-κB Signaling. International Journal of Molecular Sciences. 2022; 23: 6354.
42. Zare N, Motamedi F, Digaleh H, Khodagholi F, Maghsoudi N. Collaboration of geldanamycin-activated P70S6K and Hsp70 against beta-amyloid-induced hippocampal apoptosis: an approach to long-term memory and learning. Cell Stress and Chaperones. 2015; 20: 309-19.
43. Taylor PR, Tsoni SV, Willment JA, Dennehy KM, Rosas M, Findon H, et al. Dectin-1 is required for beta-glucan recognition and control of fungal infection. Nature immunology. 2007; 8: 31-8.
44. Worth D, Nance JP, Jang J, David C, Nair M, Wilson E. A role for dectin-1 in the CNS during chronic Toxoplasma gondii infection (MPF5P.739). 2015.
45. Deerhake ME, Danzaki K, Inoue M, Cardakli ED, Nonaka T, Aggarwal N, et al. Dectin-1 limits autoimmune neuroinflammation and promotes myeloid cell-astrocyte crosstalk via Card9-independent expression of Oncostatin M. Immunity. 2021; 54: 484-98 e8.
46. Rodríguez-Gómez JA, Kavanagh E, Engskog-Vlachos P, Engskog MK, Herrera AJ, Espinosa-Oliva AM, et al. Microglia: agents of the CNS pro-inflammatory response. Cells. 2020; 9: 1717.
47. Peng Y, Condello C, Keene CD, Wang Y, Bird T, Paul S, et al. TREM2 Haplodeficiency in Mice and Humans Impairs the Microglia Barrier Function Leading to Decreased Amyloid Compaction and Severe Axonal Dystrophy. Neuron. 2016; 90: 724-39.
48. Ulrich JD, Finn MB, Wang Y, Shen A, Mahan TE, Hong J, et al. Altered microglial response to Aβ plaques in APPPS1-21 mice heterozygous for TREM2. Molecular Neurodegeneration. 2014; 9.
49. Frank S, Burbach GJ, Bonin M, Walter M, Deller T. TREM2 is upregulated in amyloid plaque-associated microglia in aged APP23 transgenic mice. Glia. 2010; 56: 1438-47.
50. Jay TR, Hirsch AM, Broihier ML, Miller CM, Neilson LE, Ransohoff RM, et al. Disease Progression-Dependent Effects of TREM2 Deficiency in a Mouse Model of Alzheimer's Disease. J Neurosci. 2017; 37: 637-47.
51. Deerhake ME, Shinohara ML. Emerging roles of Dectin-1 in noninfectious settings and in the CNS. Trends in immunology. 2021; 42: 891-903.